OPTIMIZATION OF STEERING ELEMENTS IN THE RIA DRIVER LINAC*

E. S. Lessner [#], V. S. Assev and P. N. Ostroumov
Argonne National Laboratory, Argonne, IL 60439, USA

Abstract

The driver linac of the projected RIA facility is a versatile accelerator, a 1.4-GV, CW superconducting (SC) linac designed to simultaneously accelerate several heavy-ion charge states, providing beams from proton to uranium at 400 MeV/u at power levels at a minimum of 100 kW and up to 400 kW for most beams. Acceleration of multiple-charge-state uranium beams places stringent requirements on the linac design. A steering algorithm was derived that fulfilled the driver's real estate requirements, such as placement of steering dipole coils on SC solenoids and of beam position monitors outside cryostats, and beam-dynamics requirements, such as coupling effects induced by the focusing solenoids. The algorithm has been fully integrated into the tracking code TRACK and it is used to study and optimize the number and position of steering elements that minimize the multiple-beam centroid oscillations and preserve the beam emittance under misalignments of accelerating and transverse focusing elements in the driver linac.

DRIVER REQUIREMENTS

The RIA driver linac will accelerate enough current to deliver 400 kW of beam power to the facility target area. The driver will also accelerate ions from protons to uranium at energies of 400 MeV/nucleon [1]. For the heaviest ions, simultaneous acceleration of multi-charged-states of the stripped ions will provide enough current and overcome the present ion source limitations. Two strippers will provide the optimal charge states to attain the 400 MeV/u with a reduced linac length. Given the high power of the beam extremely low levels of losses, ~ 1 W/m must be achieved, so that hands-on-maintenance and low machine down-time be attainable. Low losses are achieved by providing large transverse and longitudinal acceptances, requiring corrective steering of the bunch centroid in all phase space planes. Beam loss can also result from emittance growth due to misaligned lattice components such as cavities and focusing magnets and must be corrected. A correction algorithm applied to the driver must comply with real-estate limitations of very tight drift spaces and coupling introduced by solenoidal focusing elements. Details of an algorithm that fulfils the driver requirements can be found in [2]. In this paper, we present the algorithm as fully implemented in the code TRACK, a multi-purpose tracking simulation code specially suited to simulations of acceleration of heavy-ions in SC linacs [3]. The algorithm has been rewritten for

computational efficiency, and has additional features such as the assignment of accuracy and precision errors to each monitor. We present the algorithm in its new implementation and preliminary studies to optimize the number and location of steering elements in the SC driver linac.

CORRECTION ALGORITHM NEW IMPLEMENTATION

The algorithm can be implemented in "correction sections", whereby N correctors and M monitors are related by the following two sets of equations:

$$\sum_{i=1}^{N_x} R_{12}(i,i') f_x(i) + \sum_{i=1}^{N_y} R_{14}(i,i') f_y(i) = -x_{mon}(i') \qquad \text{(1-a)}$$

$$\sum_{i=1}^{N_x} R_{32}(i,i') f_x(i) + \sum_{i=1}^{N_y} R_{34}(i,i') f_y(i) = -y_{mon}(i') \qquad \text{(1-b)}$$

In Eq. 1-a, $R_{12}(i, i')$ are the transfer functions between the horizontal angle (kick) at corrector i and the horizontal position at monitor i'. R_{14} are the transfer functions between the vertical angle at corrector i and the horizontal position at monitor i' - in general, R_{14} are non-zero due to coupling; f_x and f_y are the (unknown) horizontal and vertical corrector strengths, respectively. In these equations, the transfer functions include lattice errors, and the monitor coordinates include accuracy errors. Similar notation applies to Eq. 1-b. It is convenient to rewrite Eqs. 1 in matrix form:

$$(R + \Delta R) F = - (X + \Delta X), \qquad (2)$$

where R and X represent the transport matrix and monitor vector coordinates for the ideal lattice, respectively. ΔR denotes the matrix deviations due to lattice errors (misalignments and field errors), and ΔX are errors in the monitor-coordinates vector introduced by monitor inaccuracies. The corrector strengths are then determined by minimizing the function Ω given in Eq.3. Ω includes statistical weights, w_i, useful in evaluating the correction scheme effectiveness. The minimization must obey constraints imposed by realistic limits, C, on the corrector strengths:

$$\Omega(F) = \sum_{i=1}^{2M} \left(\frac{\sum_{k=1}^{N_x+N_y} (R_{ik} + \Delta R_{ik}) F_k + X_i + \Delta X_i}{w_i} \right)^2, |F_k| \le C_k. \quad (3)$$
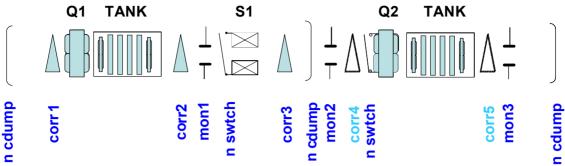
Figure 1: A possible correction section showing focusing, steering elements, and tanks, or cryostats, containing accelerating elements. The correctors in light blue correspond to correctors not used in the depicted correction section.

Figure 1 displays a typical "correction section" containing correctors, monitors, quadrupoles, and tanks containing resonators. In the figure, "cdump" area markers indicate the beginning and end of a correction section; "switch" is a zero-length device which allows changes in field strength of focusing elements located immediately downstream. This option provides a new set of transport equations for the region delimited, and is very useful in improving the correction scheme effectiveness. It is a faster realization of the dispersion correction method on which the algorithm is based [4]

The beam slope coordinates can also be corrected, by introducing a virtual monitor a distance L away from the real monitor where one wants to determine the beam-centroid angle. In this case, two additional equations, similar to Eqs.1, are introduced, containing transfer functions relating the slopes at the correctors to the slopes at the monitors, including coupling terms. Finally, the new algorithm implementation has shown to be two to three orders of magnitude faster than the original one.

AN OPTIMIZED STEERING LATTICE

The driver consists of three sections, designated low-, medium-, and high-energy sections, separated by two stripper areas. For an effective minimization, it is necessary to divide each linac sector into *correction sections*. The corrected beam from an upstream section is input to a downstream section subject to errors, which is then corrected.

The low-energy section precedes the first stripper. There are ten cryo-modules in this part of the driver, and focusing is provided by SC solenoids, of lengths from 10 cm to 30 cm. For correction purposes, the low-energy section is subdivided into three correction sections. In the first two cryostats, where the energy is very low, two correctors in each cryostat are necessary to ensure proper steering. In the remaining of the low-energy section, one corrector per cryostat is sufficient to steer the beam. In the medium-energy section following the first stripper, five charge-states are accelerated simultaneously. In this section of the driver there are 21 cryostats and 30-cm long SC solenoids,

varying from 4.5 Tesla to ~7 Tesla. It is subdivided into three correction sections, with one corrector and one monitor per cryostat providing good steering. In the low- and medium-energy driver sections steering will be effected by dipole coils mounted on solenoids, inside the cryostats. In our present simulations, correctors are represented by thin-elements. In the baseline option of the high-beta section, which comes after the second stripper, transverse focusing is provided by 42 pairs of warm quadrupoles. Elliptical cavities, of geometrical ß equal to 0.49, 0.69 and 0.81, are distributed in 43 periods. There are two correction sections where, except for the first two cryostats, one corrector every other cryostat and one monitor after each cryostat are sufficient to steer the beam. Table 1 displays the number of resonators, focusing and steering elements distributed in the three SC driver linac sections.
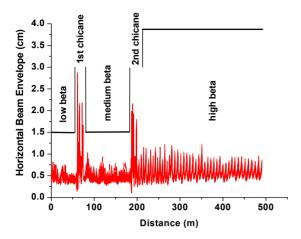
Table 1: Steering elements distribution in the three SC driver sections. Accelerating and focusing components are also shown.

Element	Low En.	Med. En.	High En.
Resonator	83	184	172
Solenoid	40	45	0
Quadrupole	0	0	84
Corrector	13	19	22
Monitor	7	18	41

In the following, results from 60-seeds simulations with 40,000 macro particles each are shown for corrections employing the aforementioned correction scheme. Simulations were carried for random-uniform resonator misalignments of 0.05-cm, solenoid misalignments varying from 0.015 for the shortest solenoids up to 0.05-cm for the longest solenoids, and quadrupole misalignments of 0.02 cm. Monitor precision errors were set at 100 μm.

Figure 2 depicts the corrected horizontal beam envelope, shown on the top, and the horizontal beam centroid., shown on the bottom. As can be seen, the corrected envelope is well below the pipe radius; shown schematically. The large

spikes in the figure correspond to the stripper locations. The beam centroid oscillations are within ~ ± 0.3 cm.
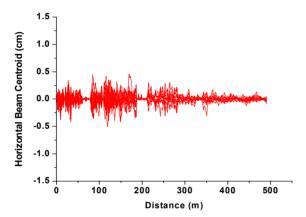

Figure 2: Corrected horizontal envelope (top), where the aperture radius is indicated, and beam centroid (bottom) for 60 seeds, under misalignments described in the text.

In Fig. 3, the integrated corrector strength distributions over 60 seeds are shown. The horizontal distribution is slightly more spread that the vertical distribution; however, all corrector strengths are within estimated acceptable limits. Figure 4 shows the corrected beam centroid coordinate distributions, where a few outliers are present in the horizontal distribution.
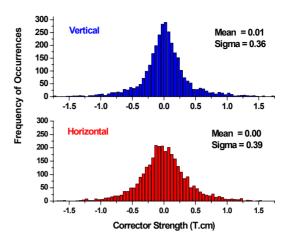

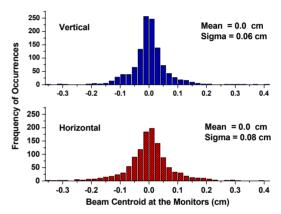Figure 3: Vertical (top) and horizontal (bottom), corrector strength distributions over 60 seeds.

Figure 4: Vertical (top) and horizontal (bottom) distributions of the corrected monitor coordinates.

SUMMARY

A 4D minimization algorithm tailored to multiple-beam steering can correct position and angle and account for solenoid-induced couplings. It is a beam-based algorithm and amenable to be implemented experimentally. It has been optimized for computational efficiency in its full integration in TRACK. It is being used to optimize the number and position of correcting elements in the RIA driver linac. Additional features will include a realization of correction by dipole coils mounted on solenoids and automatic evaluation of correction scheme effectiveness.

REFERENCES

[1] J. A. Nolen, Nucl. Phy. A. **734,** p. 661 (2004).
[2] E. S. Lessner and P. N. Ostroumov, EPAC04 Proceedings (2004), p. 1476.
[3] P.N. Ostroumov, V. S. Aseev, E. S. Lessner, B. Mustapha, these Proceedings.
[4] T. O. Raubenheimer and R. D. Ruth, SLAC-PUB-5222 (2002).